Supplementary Information

S1. Mathematical modelling

The dynamics of the SLUG circuit describes the dynamics of the molecular species of the EMT regulatory circuit (miR-200, Snail, Zeb) and SLUG as shown in Fig 2A. This set-up extends the mathematical model of EMT circuit previously developed (1). The following set of coupled ordinary differential equations (ODEs) represent the dynamics of the species of the circuit (External signal: I, miR-200: μ_{200}, SNAIL: S, ZEB: Z, SLUG: Sl):

$$\frac{d\mu_{200}}{dt} = g_{\mu_{200}} H^s(Z,\lambda_{Z,\mu_{200}}) H^s\left(S,\lambda_{S,\mu_{200}}\right) H^s\left(Sl,\lambda_{Sl,\mu_{200}}\right) - m_Z Y_\mu(\mu_{200}) - m_{Sl} Y_\mu(\mu_{200}) - k_{\mu_{200}}\mu_{200}$$

$$\frac{dm_Z}{dt} = g_{m_Z} H^s(Z,\lambda_{Z,m_Z}) H^s\left(S,\lambda_{S,m_Z}\right) - m_Z Y_Z(\mu_{200}) - k_{m_Z} m_Z$$

$$\frac{dZ}{dt} = g_Z m_Z L(\mu_{200}) - k_Z Z$$

$$\frac{dS}{dt} = g_S H^s(I,\lambda_{I,S}) H^s(Sl,\lambda_{Sl,S}) H^s\left(S,\lambda_{S,S}\right) - k_S S$$

$$\frac{dm_{Sl}}{dt} = g_{m_{Sl}} H^s\left(S,\lambda_{S,m_{Sl}}\right) - m_{Sl} Y_Z(\mu_{200}) - k_{m_{Sl}} m_{Sl}$$

$$\frac{dSl}{dt} = g_{Sl} m_{Sl} L(\mu_{200}) - k_{Sl} Sl$$

where g_X is the corresponding innate production rate and k_X is the innate degradation rate.

$m_z L(\mu_{200})$ is the net translation rate, $m_z Y_m(\mu_{200})$ is the total ZEB mRNA active degradation rate and $m_z Y_\mu(\mu_{200})$ is the total miR active degradation rate. H^S is the shifted Hill function, defined as

$H^S(B,\lambda) = H^-(B) + \lambda H^+(B)$,

$H^-(B) = 1/\left[1+(B/B_0)^{nB}\right]$,

$H^+(B) = 1 - H^-(B)$,

λ is the fold change from the basal synthesis rate due to protein B. λ >1 for activators, while λ<1 for inhibitors. When SLUG self-activation is included, the equations of SLUG are updated to include a shifted Hill function in the $\frac{dm_{Sl}}{dt}$ (SLUG mRNA) equation.

Parameter Estimation:

The model parameters were adopted from previously published literature for the molecular species of the core circuit (I, miR-200, Snail, Zeb) and SLUG interactions, as given below:

Parameter	Value	Reference
gμ200 (Molecules/Hour)	2.1K	(1)
gmZ (Molecules/Hour)	11	(1)
$Z^0\mu_{200}$ (Molecules)	220K	(1)
$Z^0 m_Z$ (Molecules)	25K	(1)
$n_{Z,\mu_{200}}$	3	(1)
n_{Z,m_Z}	2	(1)
$n_{\mu_{200}}$	6	(1)
$n_{S,\mu_{200}}$	2	(1)

n_{S,m_Z}	2	(1)
$\lambda_{Z,\mu_{200}}$	0.1	(1)
λ_{Z,m_Z}	7.5	(1)
$\lambda_{S,\mu_{200}}$	0.1	(1)
λ_{S,m_Z}	10	(1)
$k_{\mu_{200}}$(Hour^{-1})	0.05	(1)
k_{m_Z}(Hour^{-1})	0.5	(1)
k_Z(Hour^{-1})	0.1	(1)
g_Z(Hour^{-1})	0.1K	(1)
$S^0_{\mu_{200}}$(Molecules)	180K	(1)
$S^0_{m_Z}$(Molecules)	180K	(1)
μ^0_{200}(Molecules)	10K	(1)
g_S	18000	(1)
k_S	0.125	(1)
g_{Sl}	50000	Estimated
k_{Sl}	0.1155	(2)
$g_{m_{Sl}}$	90	Estimated
$k_{m_{Sl}}$	0.5	Estimated
$\lambda_{Sl,\mu_{200}}$	0.4	(3)
$\lambda_{Sl,S}$	0.5	(4)
$\lambda_{Sl,m_{Sl}}$	4	(5)
$\lambda_{S,S}$	0.4	(6)
$\lambda_{S,m_{Sl}}$	0.5	(4)
$n_{Sl,\mu_{200}}$	1	(3)
$n_{Sl,S}$	3	(7)
$n_{Sl,m_{Sl}}$	4	(5)
$n_{S,S}$	5	(7)
$n_{S,m_{Sl}}$	1	(7)
$Sl^0_{\mu_{200}}$	220000	Estimated
Sl^0_S	225000	Estimated
$Sl^0_{m_{Sl}}$	250000	Estimated
S^0_S	180000	Estimated
$S^0_{m_{Sl}}$	180000	Estimated
nIs	2	(8)
I^0S	100000	(8)
$\lambda_{I,S}$	3	(8)

Table S1: Parameter values used for simulations

The details of each link used in the network can be found in Table S2.

Interaction	Reference
ZEB represses miR200	(9)
miR200 represses ZEB	(9)
SNAIL represses itself	(6)

SNAIL activates ZEB	(10)
SNAIL represses E-cad	(11)
ZEB represses E-cad	(12)
E-cad inhibits β-catenin	(13)
β-catenin activates ZEB	(14)
SLUG self activates	(5)
SLUG and miR200 mutually inhibit each other	(3)
SLUG inhibits E-cad	(15)
SLUG and SNAIL mutually inhibit each other	(4)
ZEB self activates	(16)
SNAIL represses miR200	(17)

Table S2: References for specific nodes and links in the network

Supplementary figures:

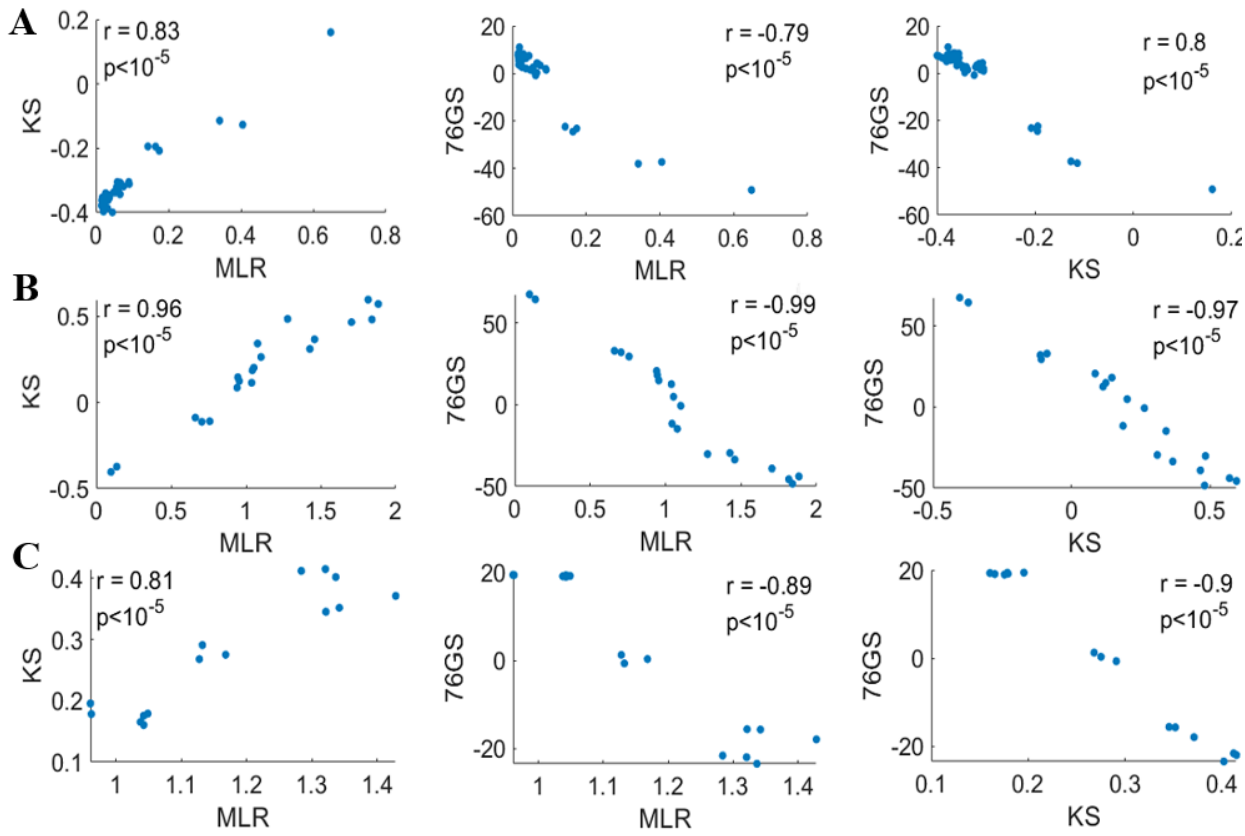

Fig S1: **Correlation plots among EMT scoring methods – KS, 76GS, MLR**. **A)** Spearman's correlation plots between KS, MLR and 76GS methods for GSE80042. **B)** Same as A) but for GSE40690. **C)** Same as A) but for GSE43495. Correlation coefficient is denoted by r, p-value is denoted by p.

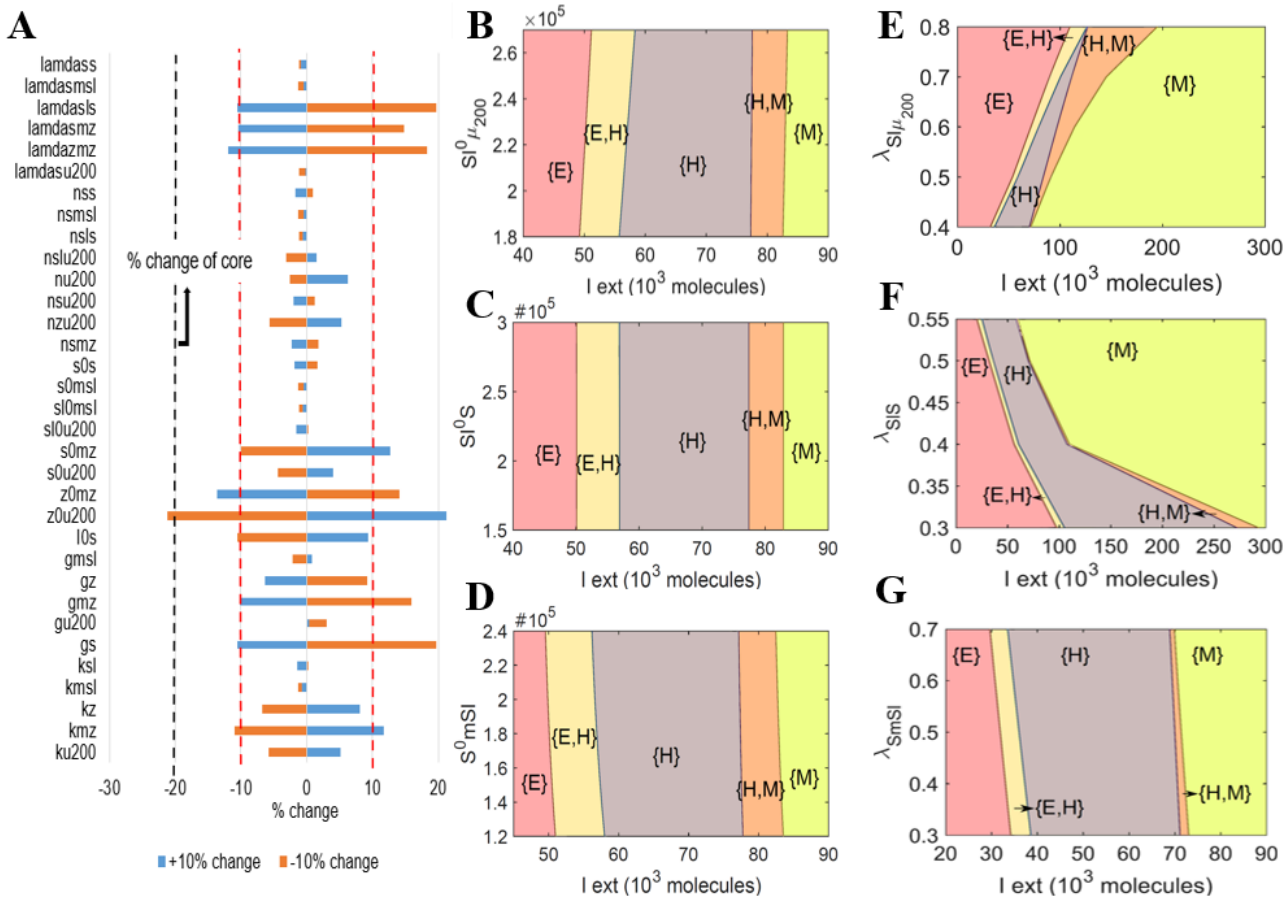

Fig S2: **Sensitivity analysis. A)** Sensitivity analysis indicating percentage change in the interval of external signal levels for the existence of stable hybrid E/M region, when corresponding parameter values are varied by ±10%. Black dotted line indicates the percent change in the stable hybrid region in the absence of SLUG (core network) when compared to the network that includes SLUG. **B)** Phase diagram of network including SLUG, when driven by external signal (I) and varying threshold of SLUG level for miR200 inhibition. **C)** Phase diagram of the SLUG network when driven by external signal (I) and varying threshold of SLUG level for SNAIL inhibition. **D)** Phase diagram of the SLUG network when driven by external signal (I) and varying threshold of SNAIL levels for SLUG mRNA inhibition. **E)** Same as Fig 2C, i but in presence of SLUG self-activation. **F)** Same as Fig 2D, i but in the presence of self-activation. **G)** Same as Fig 2D, ii but in the presence of SLUG self-activation. Parameters for SLUG self-activation are given in SI Table 1.

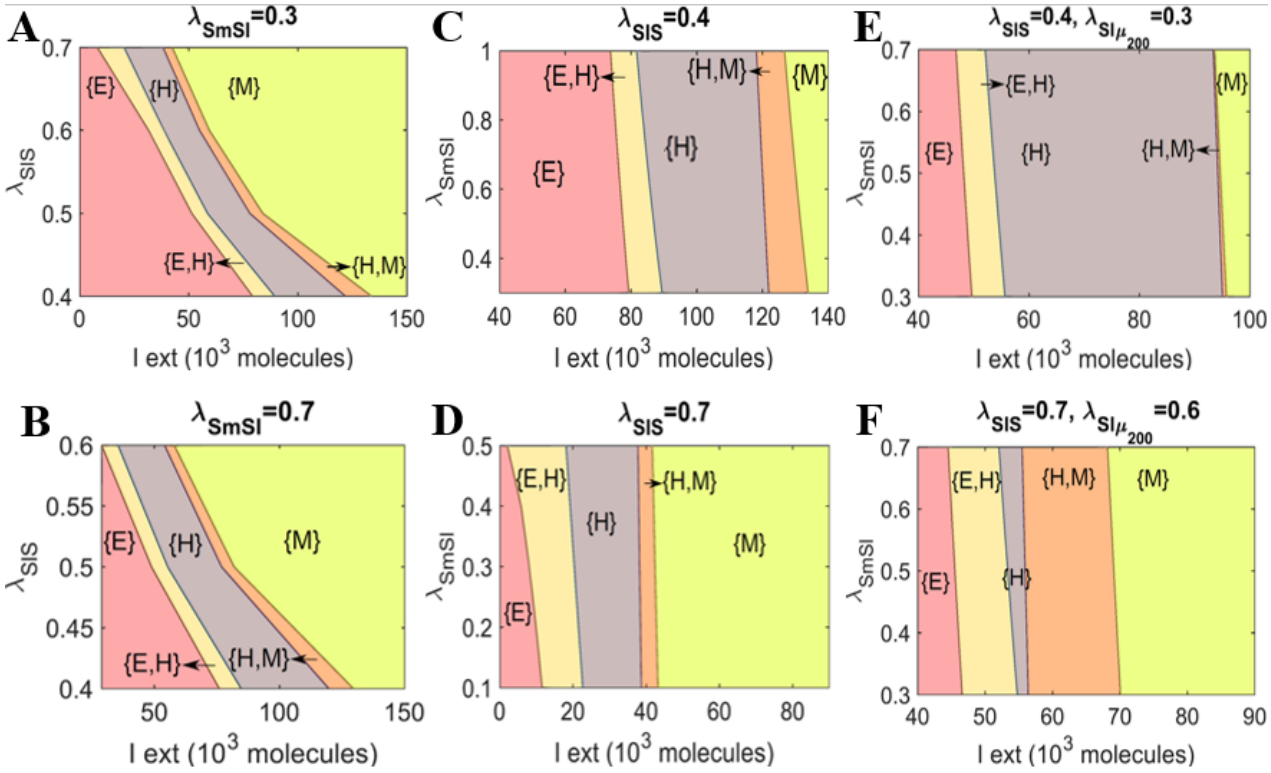

Fig S3: **Phase diagrams of the network including SLUG**. **A)** Phase diagram of SLUG network when driven by external signal (I) and varying strength of interaction between SLUG and SNAIL, under the conditions of a stronger inhibition of SLUG by SNAIL ($\lambda_{S,m_{Sl}}$ = 0.3 instead of 0.5 as in Fig 2D,i). **B)** Same as A) but for $\lambda_{S,m_{Sl}}$=0.7. **C)** Phase diagram of SLUG network when driven by external signal (I) and varying strength of interaction between SLUG and SNAIL, under the conditions of a stronger inhibition of SNAIL by SLUG ($\lambda_{Sl,S}$ = 0.4 instead of 0.5 as in Fig 2D, ii). **D)** Same as C) but for $\lambda_{Sl,S}$ = 0.7. **E)** Phase diagram of SLUG network when driven by external signal (I) and varying strength of interaction between SLUG and SNAIL, under conditions of a stronger inhibition of SNAIL and miR200 by SLUG ($\lambda_{Sl,S}$ = 0.4 and $\lambda_{Sl,\mu_{200}}$=0.3 instead of 0.5 and 0.4 respectively as in Fig 2D, i). **F)** Same as E) but for weaker inhibition of SNAIL and miR-200 by SLUG $\lambda_{Sl,S}$ = 0.7 and $\lambda_{Sl,\mu_{200}}$=0.6.

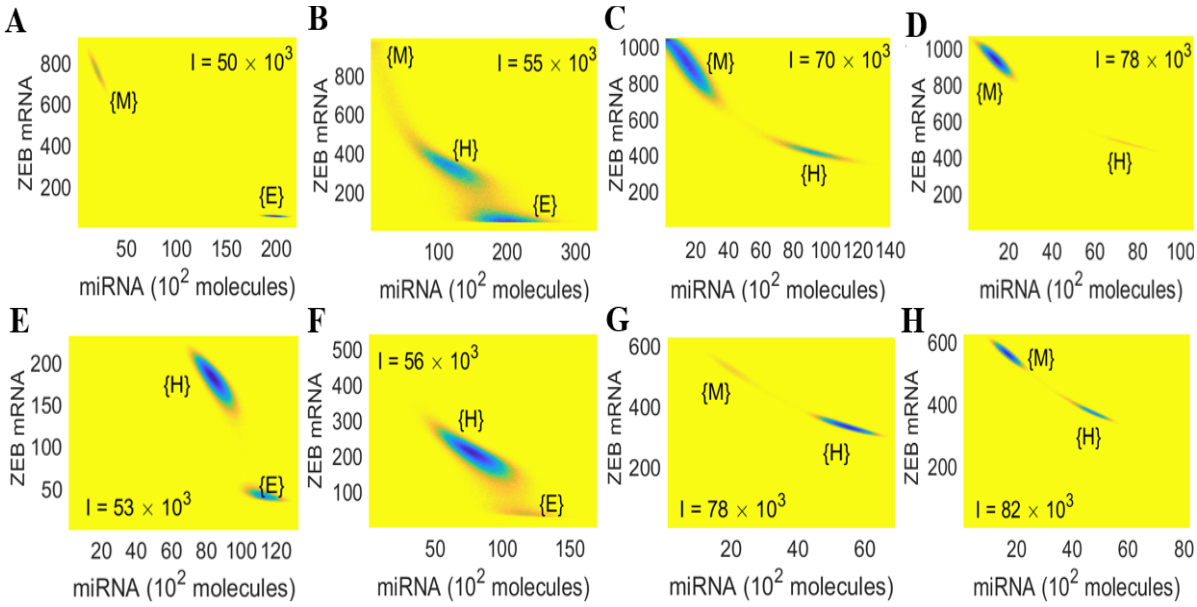

Fig S4: Potential landscape A-D) Potential landscape for core circuit at varying levels of external signal (I). **(E-H)** Potential landscape for the circuit including SLUG at varying levels of external signal (I).

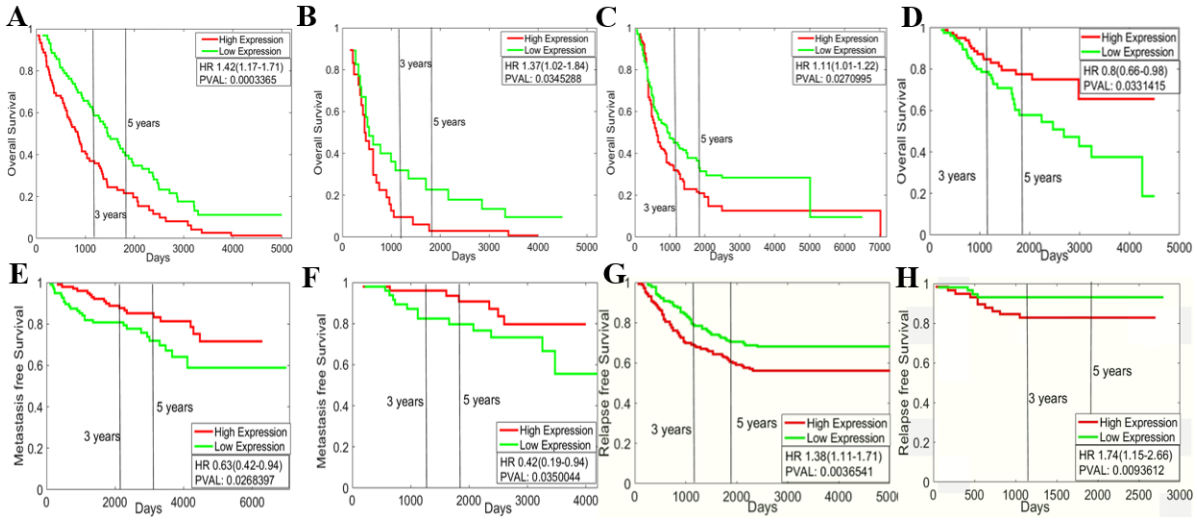

Fig S5: **Kaplan–Meier analysis for SLUG levels**. **A-D)** Overall survival of GSE26712 (ovarian cancer samples), GSE18520 (ovarian cancer sample), GSE13876 (ovarian cancer sample) and GSE3143 (breast cancer sample) respectively. **E-F)** Metastasis free survival of GSE11121 and GSE2990 (breast cancer samples) respectively. **G-H)** Relapse free survival of GSE2034 and GSE19615 (breast cancer samples) respectively. HR denotes Hazard ratio, PVAL denotes p-value.

References:

1. Lu M, Jolly MK, Levine H, Onuchic JN, Ben-Jacob E. MicroRNA-based regulation of epithelial-hybrid-mesenchymal fate determination. *Proc Natl Acad Sci U S A* (2013) **110**:18144–18149. doi:10.1073/pnas.1318192110

2. Molina-Ortiz P, Villarejo A, MacPherson M, Santos V, Montes A, Souchelnytskyi S, Portillo F, Cano A. Characterization of the SNAG and SLUG domains of Snail2 in the repression of E-cadherin and EMT induction: Modulation by serine 4 phosphorylation. *PLoS One* (2012) **7**:1–12. doi:10.1371/journal.pone.0036132

3. Liu YN, Yin JJ, Abou-Kheir W, Hynes PG, Casey OM, Fang L, Yi M, Stephens RM, Seng V, Sheppard-Tillman H, et al. MiR-1 and miR-200 inhibit EMT via Slug-dependent and tumorigenesis via Slug-independent mechanisms. *Oncogene* (2013) **32**:296–306. doi:10.1038/onc.2012.58

4. Nakamura R, Ishii H, Endo K, Hotta A, Fujii E, Miyazawa K, Saitoh M. Reciprocal expression of slug and snail in human oral cancer cells. *PLoS One* (2018) **13**:1–14. doi:10.1371/journal.pone.0199442

5. Kumar B, Uppuladinne MVN, Jani V, Sonavane U, Joshi RR, Bapat SA. Auto-regulation of Slug mediates its activity during epithelial to mesenchymal transition. *Biochim Biophys Acta - Gene Regul Mech* (2015) **1849**:1209–1218. doi:10.1016/j.bbagrm.2015.07.006

6. Peiró S, Escrivà M, Puig I, Barberà MJ, Dave N, Herranz N, Larriba MJ, Takkunen M, Francí C, Muñoz A, et al. Snail1 transcriptional repressor binds to its own promoter and controls its expression. *Nucleic Acids Res* (2006) **34**:2077–2084. doi:10.1093/nar/gkl141

7. Chen Y, Gridley T. The SNAI1 and SNAI2 proteins occupy their own and each other's promoter during chondrogenesis. *Biochem Biophys Res Commun* (2013) **435**:356–360. doi:10.1016/j.bbrc.2013.04.086

8. Jolly MK, Boareto M, Debeb BG, Aceto N, Farach-Carson MC, Woodward WA, Levine H. Inflammatory Breast Cancer: a model for investigating cluster-based dissemination. *NPJ Breast Cancer* (2017) **3**:21. doi:https://doi.org/10.1101/119479

9. Burk U, Schubert J, Wellner U, Schmalhofer O, Vincan E, Spaderna S, Brabletz T. A reciprocal repression between ZEB1 and members of the miR-200 family promotes EMT and invasion in cancer cells. *EMBO Rep* (2008) **9**:582–589. doi:10.1038/embor.2008.74

10. Guaita S, Puig I, Francí C, Garrido M, Domínguez D, Batlle E, Sancho E, Dedhar S, De Herreros AG, Baulida J. Snail induction of epithelial to mesenchymal transition in tumor cells is accompanied by MUC1 repression and ZEB1 expression. *J Biol Chem* (2002) **277**:39209–39216. doi:10.1074/jbc.M206400200

11. Batlle E, Sancho E, Francí C, Domínguez D, Monfar M, Baulida J, De Herreros AG. The transcription factor Snail is a repressor of E-cadherin gene expression in epithelial tumour cells. *Nat Cell Biol* (2000) **2**:84–89. doi:10.1038/35000034

12. Singh AB, Sharma A, Smith JJ, Krishnan M, Chen X, Eschrich S, Washington MK, Yeatman TJ, Beauchamp RD, Dhawan P. Claudin-1 up-regulates the repressor ZEB-1 to inhibit E-cadherin expression in colon cancer cells. *Gastroenterology* (2011) **141**:2140–2153. doi:10.1053/j.gastro.2011.08.038

13. Orsulic S, Huber O, Aberle H, Arnold S, Kemler R. E-cadherin binding prevents β-catenin nuclear localization and β-catenin/LEF-1-mediated transactivation. *J Cell Sci*

(1999) **112**:1237–1245.

14. Tan Y-F, Tang L, OuYang W-X, Jiang T, Zhang H, Li S-J. β-catenin-coordinated lncRNA MALAT1 up-regulation of ZEB-1 could enhance the telomerase activity in HGF-mediated differentiation of bone marrow mesenchymal stem cells into hepatocytes. *Pathol - Res Pract* (2019) **215**:546–554. doi:10.1016/j.prp.2019.01.002

15. Hajra KM, Chen DYS, Fearon ER. The SLUG zinc-finger protein represses E-cadherin in breast cancer. *Cancer Res* (2002) **62**:1613–1618.

16. Hill L, Browne G, Tulchinsky E. ZEB/miR-200 feedback loop: At the crossroads of signal transduction in cancer. *Int J Cancer* (2012) **132**:745–754. doi:10.1002/ijc.27708

17. Gill JG, Langer EM, Lindsley RC, Cai M, Murphy TL, Kyba M, Murphy KM. Snail and the microRNA-200 family act in opposition to regulate epithelial-to-mesenchymal transition and germ layer fate restriction in differentiating ESCs. *Stem Cells* (2011) **29**:764–776. doi:10.1002/stem.628